The 7th World Conference on Structural Control and Monitoring, 7WCSCM,
July 22-25, 2018, Qingdao, China

Observability and Identification of Damage-Healing Hysteretic Model

X. Shi[a], M.N. Chatzis[a], S.P. Triantafyllou[b] & M.S. Williams[a]

[a] Department of Engineering Science, University of Oxford, Oxford, UK
[b] Department of Civil Engineering, University of Nottingham, Nottingham, UK

Abstract: Recent advances in the development of self-healing materials have highlighted the need for accurate modelling of the self-healing mechanism. To this end, the damage-healing hysteretic model is derived to describe the nonlinear behaviour of structures with self-healing material by introducing additional operators to the Bouc-Wen model. When the model is used as a representation of a real structure, it is important to precisely identify the model parameters to reduce the pertaining uncertainties. In this work, the nonlinear observability methods and the concept of non-smooth observability are utilized to analyze the observability of the model. The Unscented Kalman filter (UKF) and the recently suggested Discontinuous Unscented Kalman filter (DUKF) are implemented to identify the model, and the superior performance of the DUKF for parametric identification of non-smooth systems is highlighted.

1 Introduction

The Bouc-Wen model of hysteresis is commonly utilized to account for nonlinear behaviour of structures [1]. Over the past decades, earthquake demand studies have motivated the development and modification of the Bouc-Wen model to make it capable of representing various modes of structural damage such as stiffness degradation, strength deterioration and the pinching effect [2,3]. However, for a specific model representation of a real structure, the model parameters that are related to the structural properties, such as the stiffness and damping, often remain uncertain or unknown. One of the means to estimate the model parameters is through placing sensors on the structure to measure its vibrational data and then using system identification methods on the measurements [4,5]. Accurate estimation of the parameters improves engineers' confidence in the theoretical model for a real structure that can then be used in numerical simulation, health assessment and earthquake risk estimation.

Development of novel self-healing materials has gained increasing attention in recent years, while a lot of research has been performed on the engineering materials with self-healing property such as concrete, asphalt and mortar. For better modelling the self-healing mechanism, Triantafyllou et al. [6-8] extended the generalized Bouc-Wen model to a damage-healing hysteretic model by introducing additional operators to describe how the damage evolves based on the hysteretic energy accumulation, and how the damage is recovered considering the property of self-healing material. The damage-healing hysteretic model is important as it enables engineers to have a better understanding of the behaviour of structures with self-healing material when subject to the effect of either gradual deterioration or extreme loading. However, identification of such a hysteretic model becomes much more challenging, because the additional operators and parameters substantially increase the nonlinearity and discontinuity of the model equations.

A priori observability analysis of a dynamic system, that is, to explore whether the parameters and dynamic states of the system can be identified and tracked with respect to particular input and output measurements, is a necessary step before identification. Several observability approaches to nonlinear systems, such as the geometric Observability Rank Condition (ORC) [9] and the algebraic Observability Test [10], have been developed for different forms of differentiable nonlinearities. In the case of non-smooth systems i.e. systems with non-differentiable equations, Chatzis et al. discussed their observability in [11] by dividing a non-smooth system into several smooth subsystems and thus enabling observability methods to be employed separately for each of the subsystems. The Unscented Kalman filter (UKF) based on the unscented transform is a robust online identification algorithm for parametric estimation. Following the work on the non-smooth observability, Chatzis et al. [12] suggested a novel algorithm, termed the Discontinuous Unscented Kalman filter (DUKF), in order to optimize the performance of the UKF particularly for non-smooth systems.

This work aims to seek an efficient way to identify the damage-healing hysteretic model. A dynamic system of a mass connected with a damage-healing spring and a linear damper is investigated. The observability of the investigated system is studied by the ORC and the Observability Test, and based on the observability results the system is transformed into a modified version where all the involved parameters and states are observable. The occurring modified system is identified using both the UKF and the DUKF, illustrating the advantages of applying the D-modification to this problem, as well as the ability to properly identify the properties of such a system from a suitably chosen numerical experiment.

2 Damage-Healing Hysteretic Model

2.1. Constitutive formulation

The triaxial hysteretic formulation is considered herein to characterize the elastic and inelastic behaviour of the investigated model [7,8]. The formulation mainly consists of two evolution equations that are derived from the principles of the additive decomposition of strain rates, the flow rule, the kinematic hardening law and the consistency condition. They are the total stress evolution and the backstress evolution:

$$\{\dot{\sigma}\} = [D]([I] - H_1 H_2 [R])\{\dot{\varepsilon}\}, \quad \{\dot{\eta}\} = H_1 H_2 G(\{\eta\}, \Phi)[\tilde{R}]\{\dot{\varepsilon}\} \tag{1}$$

where $\{\sigma\}$ is the stress tensor, $\{\eta\}$ is the backstress tensor, $\{\varepsilon\}$ is the total strain tensor, $[D]$ is the elastic constitutive matrix, $[I]$ is a 6×6 identity matrix and Φ is the yield surface. $[R]$ is the projection of the plastic strain tensor onto the total strain tensor, defined as:

$$[R] = \frac{\partial\Phi}{\partial\{\sigma\}}[\tilde{R}], \quad [\tilde{R}] = (-\left(\frac{\partial\Phi}{\partial\{\eta\}}\right)^T G(\{\eta\},\Phi) + \left(\frac{\partial\Phi}{\partial\{\sigma\}}\right)^T [D]\frac{\partial\Phi}{\partial\{\sigma\}})^{-1}\left(\frac{\partial\Phi}{\partial\{\sigma\}}\right)^T [D] \tag{2}$$

H_1 and H_2 are defined as continuous functions of the yield function and the stress field:

$$H_1 = \left|\frac{\Phi}{\Phi_0}\right|^N, N \geq 1, \quad H_2 = \beta + \gamma sgn(\left(\frac{\partial\Phi}{\partial\{\sigma\}}\right)^T \{\dot{\sigma}\}) \tag{3}$$

where N, β and γ are the model parameters, and Φ_0 is the maximum value of the yield function. G is the kinematic hardening function where the Armstrong-Frederick (AF) model is used:

$$G(\{\eta\},\Phi) = \frac{2}{3}h\frac{\partial\Phi}{\partial\{\sigma\}} - c\sqrt{\frac{2}{3}\left(\frac{\partial\Phi}{\partial\{\sigma\}}\right)^T \frac{\partial\Phi}{\partial\{\sigma\}}}\{\eta\} \tag{4}$$

where h/c is the saturated value of the backstress.

In [6], damage evolution equations that are associated with stiffness degradation and strength deterioration are introduced to the stress-strain relation. In this work, only the stiffness degradation is taken into account:

$$\{\dot{\sigma}\} = \frac{1}{v_\eta}[D]([I] - H_1 H_2 [R])\{\dot{\varepsilon}\}, \quad v_\eta = 1.0 + c_\eta E_h \tag{5}$$

where v_η is a degradation parameter derived by assuming the degradation evolves linearly with the hysteretic energy with a unity initial value. c_η is a material parameter, and E_h is the hysteretic energy of the i^{th} micro-element. In addition, the fundamental property of self-healing material is formulized as h_s to partially offset the effect of the stiffness degradation:

$$\{\dot{\sigma}\} = \frac{h_s}{v_\eta}[D]([I] - H_1 H_2 [R])\{\dot{\varepsilon}\}, \quad h_s = 1 + w_h(v_\eta - 1)\frac{1+sgn((\frac{\partial \Phi}{\partial\{\sigma\}})^T\{\dot{\sigma}\})}{2} \tag{6}$$

where w_h is the healing effectiveness parameter that is assumed to be time-independent.

2.2. Mass-spring-damper system

In this work, the investigated model is a mass-spring-damper system as shown in Figure 1.

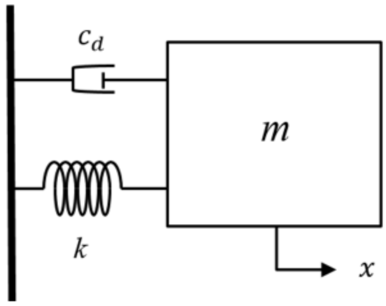

Figure 1. Mass-spring-damper system

If the excitation applied to the body is an earthquake, the equation of motion of the dynamic system can be established as follows:

$$m\ddot{x} + c_d\dot{x} + f_S = -\ddot{x}_g m, \quad f_S = A\sigma \tag{7}$$

where x is the relative displacement of the body with respect to the ground, m is the mass of the body, c_d is the damping coefficient and $\ddot{x}_g$ is the ground acceleration. f_S is the restoring force of the uniaxial spring element, where A is the cross-section area of the spring element, and σ is the stress, whose dynamic evolution follows the damage-healing hysteretic formulation (6). A von Mises type of yield criterion is considered, leading the function of the yield surface and its critical value to be:

$$\Phi = (\sigma - \eta)^2, \quad \Phi_0 = {\sigma_y}^2 \tag{8}$$

where σ_y is the yield strength. The accumulated plastic dissipated energy E_h is regarded as a time-variant dynamic state, which can be evaluated by integrating the product of stress and plastic strain rate over time. Therefore, the increasing rate of E_h is:

$$\dot{E}_h = \sigma\dot{\varepsilon}_{pl} = \sigma H_1 H_2 R\dot{\varepsilon} \tag{9}$$

Combining all of the above equations gives a complete state space representation (10) of the dynamic system where the evolution equations of all dynamic states, including the displacement of the body denoted by x_1, the velocity denoted by x_2, the stress σ, the backstress η and the hysteretic energy E_h, have been established.

$$\dot{x}_1 = x_2, \quad \dot{x}_2 = -\frac{A}{m}\sigma - \frac{c_d}{m}x_2 - \ddot{x}_g \tag{10}$$

$$\dot{\sigma} = \frac{1+w_h c_\eta E_h^{\frac{1+sgn((\sigma-\eta)x_2)}{2}}}{1+c_\eta E_h} E \cdot (1 - \left(\beta + \gamma sgn\left((\sigma-\eta)x_2\right)\right)(\frac{\sigma-\eta}{\sigma_y})^{2N} \frac{E}{\frac{2}{3}h - \frac{2^{\frac{1}{2}}}{3}c\eta \cdot sgn(\sigma-\eta) + E}) \frac{x_2}{L}$$

$$\dot{\eta} = \left(\beta + \gamma sgn\left((\sigma-\eta)x_2\right)\right)(\frac{\sigma-\eta}{\sigma_y})^{2N} \frac{\frac{2}{3}h - \frac{2^{\frac{1}{2}}}{3}c\eta \cdot sgn(\sigma-\eta)}{\frac{2}{3}h - \frac{2^{\frac{1}{2}}}{3}c\eta \cdot sgn(\sigma-\eta) + E} E \frac{x_2}{L}$$

$$\dot{E}_h = \sigma \left(\beta + \gamma sgn\left((\sigma-\eta)x_2\right)\right)(\frac{\sigma-\eta}{\sigma_y})^{2N} \frac{E}{\frac{2}{3}h - \frac{2^{\frac{1}{2}}}{3}c\eta \cdot sgn(\sigma-\eta) + E} \frac{x_2}{L}$$

where in a one-dimensional uniaxial spring element the $[D]$ is the Young's modulus E, and the total strain rate $\dot{\varepsilon}$ can be calculated from dividing the velocity x_2 by the length of the spring L. It should be noted that in the function $sgn(\left(\frac{\partial \Phi}{\partial\{\sigma\}}\right)^T \{\dot{\sigma}\})$, $\frac{\partial \Phi}{\partial\{\sigma\}}$ can be calculated since the function of Φ is known in (8). It is further considered that stiffness of the system is always positive so that the signs of $\dot{\sigma}$ and $\dot{\varepsilon}$ are always consistent. Hence, implicit equations are avoided for convenience of simulation, and the following relation holds:

$$sgn\left(\left(\frac{\partial \Phi}{\partial\{\sigma\}}\right)^T \{\dot{\sigma}\}\right) = sgn(2(\sigma-\eta)\cdot\dot{\varepsilon}) = sgn\left(2(\sigma-\eta)\cdot\frac{x_2}{L}\right) = sgn((\sigma-\eta)\cdot x_2) \tag{11}$$

3 Observability Analysis

3.1. Nonlinear observability methods

The state and measurement equations of a nonlinear system can be described as:

$$\dot{x} = f(x,u), \qquad y = h(x,u) \tag{12}$$

where x is the state vector, u is a known input vector and y is the output vector respectively. f and h are nonlinear functions of x and u. In the state and parameter identification, x is an augmented vector consisting of the dynamic states of the system, x_t, and the parameters, θ, i.e. $x = [x_t \quad \theta]$. It will be considered in the following that the parameters are time-invariant, i.e. $\dot{\theta} = 0$.

Various methods have been developed to analyze the observability of different categories of nonlinear systems. The geometric Observability Rank Condition (ORC) introduced by Hermann and Krener [9] is capable of handling general nonlinearities with analytic equations, while the algebraic Observability Test developed by Sedoglavic [10] is a robust algorithm applicable to systems with rational equations. All the previous algorithms when used on a measured dynamic system, deem of whether the dynamic states of the system are observable, i.e. can be tracked given a specific measurement setup. If a state is a parameter then the algorithms allow to investigate its identifiability, i.e. whether the measurements would allow the true value of such a parameter to be identified [11,13]. An unobservable state or an unidentifiable parameter cannot be properly identified by any algorithm regardless of the quality of the used data.

Many engineering systems are non-smooth often due to the presence of discontinuous functions in their equations. The dynamics of such a system can be expressed in smooth branches where each of the branches can be independently described by an analytic state space representation which can be regarded as a subsystem of the overall system. Following the idea, Chatzis et al. [11] deduced the observability of a non-smooth system by separating it into a set of smooth subsystems:

$$\begin{gathered} \dot{x} = f_1(x,u), \text{ when } x \in R_1^n \\ \vdots \\ \dot{x} = f_l(x,u), \text{ when } x \in R_l^n \end{gathered} \tag{13}$$

where $f_i(x,u)$ is an analytic nonlinear function within R_i^n, and therefore one can separately implement the observability methods, for example the ORC, to each of the smooth subsystems.

3.2. Observability of the damage-healing hysteretic model

Suppose the relative displacement x_1 is the measured quantity and the earthquake $\ddot{x}_g$ is the known input. Given the measurement and input, it is expected to know whether the dynamic states of the system (10) are observable and its parameters are identifiable. Five dynamic states and all of the remaining time-invariant parameters in (10) are included in the augmented state vector x:

$$x = [x_1, x_2, \sigma, \eta, Eh, A_m, c_{dm}, L, E, \sigma_y, c_\eta, w_h, c, h, \beta, \gamma, N]$$

where A_m and c_{dm} are the normalized cross-area $\frac{A}{m}$ and damping coefficient $\frac{c_d}{m}$ respectively. The state space representation (10) is therefore augmented as follows:

$$\dot{x} = [\dot{x}_1, \dot{x}_2, \dot{\sigma}, \dot{\eta}, \dot{E}_h, 0,0,0,0,0,0,0,0,0,0,0,0]^T \tag{14}$$

The system (14) is obviously not analytic due to the existence of $sgn((\sigma-\eta)\cdot x_2)$ and $sgn(\sigma-\eta)$ in the equations of $\dot{\sigma}$, $\dot{\eta}$ and $\dot{E}_h$, so neither the ORC nor the Observability Test is applicable. Following the suggestion in the previous section, this non-smooth system is divided into four smooth branches: (a) when $(\sigma-\eta)>0$ and $x_2>0$, (b) when $(\sigma-\eta)>0$ and $x_2<0$, (c) when $(\sigma-\eta)<0$ and $x_2<0$, (d) when $(\sigma-\eta)<0$ and $x_2>0$.

The ORC algorithm based on symbolic computation is extremely inefficient to deal with such a complicated system because it requires significant amount of computer memory. Hence the Observability Test is first used to study the observability of the rational version of the smooth subsystems (a), (b), (c) and (d) by assuming the parameter N to be known. It should be noted that a state found to be unobservable in this simplified rational system will also be unobservable in the original system, although this is not true for observable states [11].

The Observability Test shows that for the specific measurement setup the unobservable states of the subsystems (a) and (c) are $x_{ac}^u = [\sigma, \eta, Eh, A_m, L, E, \sigma_y, c_\eta, c, h, \beta, \gamma]$ with the transcendence degree of 4, and the unobservable states of the subsystems (b) and (d) are $x_{bd}^u = [\sigma, \eta, Eh, A_m, L, E, \sigma_y, c_\eta, w_h, c, h, \beta, \gamma]$ with the transcendence degree of 5. As has been explained in [10] the number of unobservale states is different, usually greater, than the transcendence degree. The latter exhibits the number of unobservable states which if known would result in all the ramaining states being observable. It should be that the healing operator is activated only when $(\sigma-\eta)x_2$ is positive, so the healing effectiveness parameter w_h appears in the corresponding subsystems (a) and (c) but does not exist in (b) and (d), and therefore w_h is unobservable in (b) and (d).

In the following, the state equations of the smooth branches are re-organized by combining the unobservable states to eliminate them. To achieve so, σ, η and σ_y at stress-level are first transformed to their corresponding quantities at displacement-level by substituting the following relations: $r=\frac{\sigma L}{E},\ \eta'=\frac{\eta L}{E},\ r_y=\frac{\sigma_y L}{E}$. r is known as the elastic displacement. Thus L can be eliminated from the main frames of (10), and the second and third equations become:

$$\dot{x}_2=-\frac{AE}{mL}r-c_{dm}x_2-\ddot{x}_g,\quad \dot{r}=\frac{h_s}{v_\eta}\left(1-H_1\left(\frac{r-\eta'}{r_y}\right)^{2N}R\right)x_2 \tag{15}$$

where $\frac{AE}{mL}$ is essentially the normalized stiffness $k_m=\frac{k}{m}$. To eliminate the L from the fifth equation , E_h is replaced by: $E_h'=\frac{L^2}{E}E_h$. It is found that H_1 and H_2 always occur together as a product in the equations, and they can be rearranged as: $H_1H_2=\frac{\beta+\gamma sgn\left((r-\eta')x_2\right)}{r_y^{2N}}(r-\eta')^{2N}$. A close inspection of the Bouc-Wen model indicates that identification of the combination $\frac{\beta+\gamma sgn\left((r-\eta')x_2\right)}{r_y^{2N}}$ is possible, but identification of individual parameters except N is not. To this end, two new parameters are introduced: $\Delta_1=\frac{\beta+\gamma}{r_y^{2N}}$ and $\Delta_2=\frac{\beta-\gamma}{r_y^{2N}}$, to represent the combinations of β, γ, r_y and N. Furthermore, E can be completely eliminated in the fraction of G and R by substituting:$h'=\frac{h}{E}$. Finally, in order to construct a new system which is mathematically equivalent to the original one, the following combinations are introduced: $c'=\frac{c}{L}$ and $c_\eta'=\frac{E}{L^2}c_\eta$. So far the unobservable parameters E, L and two of β, γ and r_y corresponding to the 4 transcendence degree have been combined to the other states.

Now the state vector x is reduced to:

$$x=[x_1,x_2,r,\eta',E_h',k_m,c_{dm},c_\eta',w_h,c',h',\Delta_1,\Delta_2,N] \tag{16}$$

and the subsystems (a), (b), (c) and (d) are rewritten as follows:

(A): when $(r-\eta')>0$ and $x_2>0$	(B): when $(r-\eta')>0$ and $x_2<0$
$\dot{r}=\frac{1+w_hc_\eta'E_h'}{1+c_\eta'E_h'}\left(1-\Delta_1(r-\eta')^{2N}\frac{1}{\frac{2}{3}h'-\frac{2^{\frac{1}{2}}}{3}c'\eta'+1}\right)x_2$ $\dot{\eta}'=\Delta_1(r-\eta')^{2N}\frac{\frac{2}{3}h'-\frac{2^{\frac{1}{2}}}{3}c'\eta'}{\frac{2}{3}h'-\frac{2^{\frac{1}{2}}}{3}c'\eta'+1}x_2$ $\dot{E}_h'=r\Delta_1(r-\eta')^{2N}\frac{1}{\frac{2}{3}h'-\frac{2^{\frac{1}{2}}}{3}c'\eta'+1}x_2$	$\dot{r}=\frac{1}{1+c_\eta'E_h'}\left(1-\Delta_2(r-\eta')^{2N}\frac{1}{\frac{2}{3}h'-\frac{2^{\frac{1}{2}}}{3}c'\eta'+1}\right)x_2$ $\dot{\eta}'=\Delta_2(r-\eta')^{2N}\frac{\frac{2}{3}h'-\frac{2^{\frac{1}{2}}}{3}c'\eta'}{\frac{2}{3}h'-\frac{2^{\frac{1}{2}}}{3}c'\eta'+1}x_2$ $\dot{E}_h'=r\Delta_2(r-\eta')^{2N}\frac{1}{\frac{2}{3}h'-\frac{2^{\frac{1}{2}}}{3}c'\eta'+1}x_2$
(C): when $(r-\eta')<0$ and $x_2<0$	(D): when $(r-\eta')<0$ and $x_2>0$

$\dot{r}=\frac{1+w_h c'_\eta E'_h}{1+c'_\eta E'_h}(1-\Delta_1(r-\eta')^{2N}\frac{1}{\frac{2}{3}h'+\frac{2^{\frac{1}{2}}}{3}c'\eta'+1})x_2$ $\dot{\eta}'=\Delta_1(r-\eta')^{2N}\frac{\frac{2}{3}h'+\frac{2^{\frac{1}{2}}}{3}c'\eta'}{\frac{2}{3}h'+\frac{2^{\frac{1}{2}}}{3}c'\eta'+1}x_2$ $\dot{E}'_h=r\Delta_1(r-\eta')^{2N}\frac{1}{\frac{2}{3}h'+\frac{2^{\frac{1}{2}}}{3}c'\eta'+1}x_2$	$\dot{r}=\frac{1}{1+c'_\eta E'_h}(1-\Delta_2(r-\eta')^{2N}\frac{1}{\frac{2}{3}h'+\frac{2^{\frac{1}{2}}}{3}c'\eta'+1})x_2$ $\dot{\eta}'=\Delta_2(r-\eta')^{2N}\frac{\frac{2}{3}h'+\frac{2^{\frac{1}{2}}}{3}c'\eta'}{\frac{2}{3}h'+\frac{2^{\frac{1}{2}}}{3}c'\eta'+1}x_2$ $\dot{E}'_h=r\Delta_2(r-\eta')^{2N}\frac{1}{\frac{2}{3}h'+\frac{2^{\frac{1}{2}}}{3}c'\eta'+1}x_2$

where the equations of $\dot{x}_1$, $\dot{x}_2$ and parameters are common for these four subsystems. An additional benefit is that the ORC with the assistance of model decomposition [14] becomes more efficient to perform accurate observability testing for the four modified subsystems respectively. For the subsystems (A) and (C), the observable states are $x_{AC}^{o}=[x_1,x_2,r,\eta',E'_h,k_m,c_{dm},c'_\eta,w_h,c',h',\Delta_1,N]$ and the unobservable parameter is $\theta_{AC}^{u}=[\Delta_2]$. For the subsystems (B) and (D), the observable states are $x_{BD}^{o}=[x_1,x_2,r,\eta',E'_h,k_m,c_{dm},c'_\eta,c',h',\Delta_2,N]$ and the unobservable parameters are $\theta_{BD}^{u}=[\Delta_1,w_h]$. All of the subsystems (A), (B), (C) and (D) can be expressed only in terms of the corresponding observable states and identifiable parameters. Finally, as explained in [15] the overall non-smooth system is observable and all parameters are identifiable, since the union of the observable states and parameters from different branches is the state vector x in (16).

4 Identification Methods

The UKF algorithm is developed by Julier and Ulhmann [16] for identification of nonlinear dynamic systems which are written in the discrete-time form [17]:

$$x_k=f(x_{k-1},u_{k-1})+w_{k-1},\quad y_k=h(x_k,u_k)+v_k \tag{17}$$

where w and v are white, zero mean, uncorrelated noise processes with known covariance matrices Q and R respectively. The UKF is based on the unscented transformation where a set of sigma points are carefully determined to represent the Gaussian distribution of the state and they are used to transform the mean and covariance of the state through the nonlinear system.

The discontinuous modification for the UKF is developed by Chatzis et al. [12] to exploit the special identifiability properties of non-smooth systems. The principal concept of the DUKF is to purposely maintain the unidentifiable parameters time-invariant, so that local divergence of the unidentifiable parameters in the corresponding branches is avoided and the overall convergence of the state vector is enhanced.

In this work, both the UKF and the DUKF are used to identify the invesitigated system with modified equations. For the DUKF it is important to remind the conditions that result in the change of observability as shown in Table 1.

Subsystems	(A), (C)	(B), (D)
Condition	$(r-\eta')x_2>0$	$(r-\eta')x_2<0$
Observable	x_1, x_2, r, η', E'_h, k_m, c_{dm}, c'_η, w_h, c', h', Δ_1, N	x_1, x_2, r, η', E'_h, k_m, c_{dm}, c'_η, c', h', Δ_2, N
Unidentifiable	Δ_2	Δ_1, w_h

Table 1. Observability of the invetigated system with modified equations

5 Results

The mass-spring-damper system as shown in Figure 1 subject to an earthquake is considered. The nonlinear dynamic behaviour of the spring element is formulated by the damage-healing hysteretic model. The state space representation of the system is that corresponding to the state in (16). The values of parameters are shown in Table 2 (Exact value).

The earthquake acceleration signal with the sampling frequency of 100Hz and the duration of 20s as shown in Figure 2(a) is obtained from the Northridge earthquake (1994) [18]. It was filtered with a low-frequency cutoff of 0.13Hz and a high-frequency cutoff of 30Hz. The system response of displacement resulting from simulation is shown in Figure 2(b). It will be assumed both the excitation (input) and displacement (output) are measured, and the input and output signals are contaminated with Gaussian white noise with 0.1% noise-to-signal RMS ratio.

The UKF and the DUKF successfully track the displacement as can be seen in Figure 2(b). The estimations of parameters from the UKF and the DUKF are shown in Figure 3(a) and Figure 3(b) respectively. Plots of ratio of the identified value over the exact value are presented such that the estimated values of parameters can be visibly compared to their true values. These values as well as the initial guesses of parameters are listed in Table 2.

Overall performance of the DUKF is clearly superior to that of the UKF. For the UKF, local divergence of some parameters, such as Δ_2, poses adverse effects on the overall convergence of not only itself but also the other parameters, such as c' and h'. This is effectively overcome

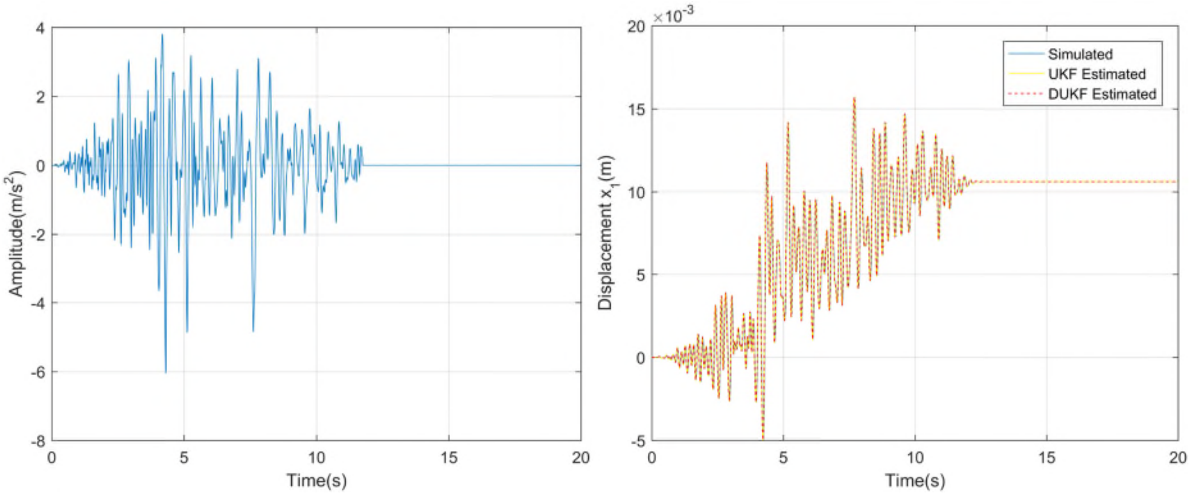

Figure 2. (a) Earthquake acceleration signal (b) Measured and estimated displacements

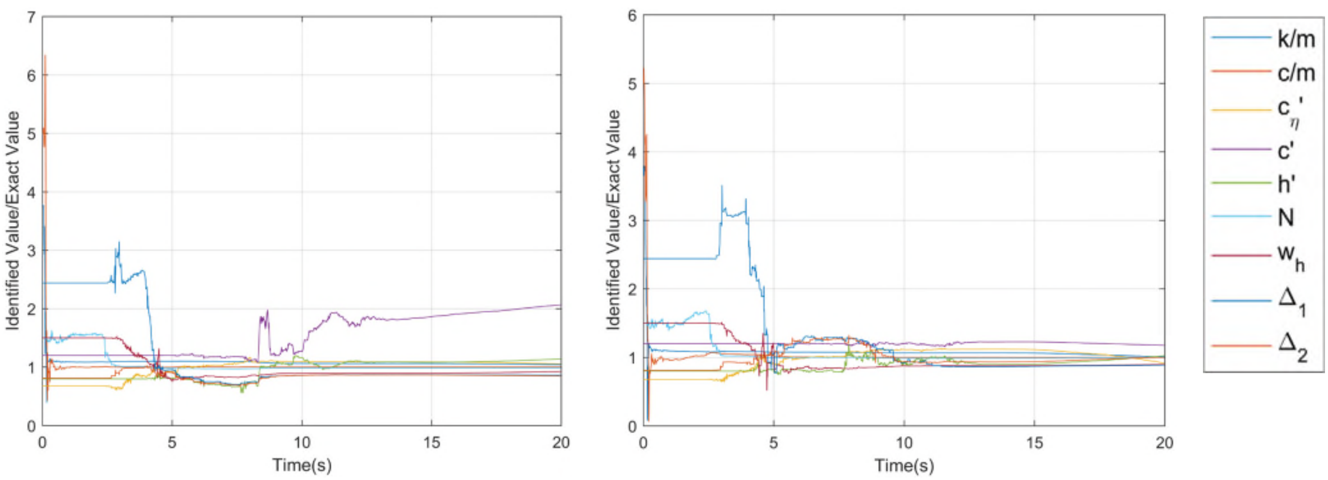

Figure 3. (a) Estimated parameters from the UKF (b) Estimated parameters from the DUKF

Method		k_m	c_m	c'_η	c'	h'	N	w_h	Δ_1	Δ_2
		$\times 10^3$	$\times 10$	$\times 10^3$	$\times 1$	$\times 10^{-3}$	$\times 1$	$\times 10^{-1}$	$\times 10^{10}$	$\times 10^9$
	Exact Value	1.33	1.00	4.44	3.33	5.00	2.00	2.00	1.23	-7.41
	Initial Guess	5	5	3	4	4	3	3	3	-6
DUKF	Estimated	1.3373	0.9999	4.0701	3.9167	5.0995	1.9996	1.7892	1.0899	-7.3951
	Error %	0.55	0.01	8.33	17.62	1.99	0.02	10.54	11.39	0.20
UKF	Estimated	1.3850	1.0002	4.6827	6.8758	5.6834	1.9744	1.8476	1.0586	-6.2759
	Error %	4.14	0.02	5.47	106.48	13.67	1.28	7.62	13.93	15.30

Table 2. Exact value, initial guess, estimated value and error of the parameters

in the DUKF by retaining the parameters constant to avoid local divergence in the corresponding branches. The parameters like w_h can still be accurately identified by the UKF as long as it converges faster in the identifiable branches than it diverges in the unidentifiable branches, as indicated in [15]. For the DUKF, one of the main identification errors is likely from the fact that at a given time the estimated subsystem used maybe different from the real subsystem because the condition of subsystem is evaluated from the estimated states rather than the real states.

6 Conclusions

The objective of this work is to efficiently identify a mass-spring-damper system where the spring element is characterized by the damage-healing hysteretic model. The damage-healing hysteretic model is recently developed in the works of Triantafyllou et al. by introducing the additional operators that formulize the fundamental properties of the self-healing material, stiffness retrieval and strength retrieval to the generalized Bouc-Wen model of hysteresis.

Based on the concept of the observability of non-smooth systems, the investigated system is divided into four smooth subsystems. Each of the subsystems is analyzed by the Observability Test and the ORC, and is modified by combining unobservable states such that the overall investigated system becomes fully observable. The UKF and the discontinous UKF (DUKF) are performed to identify the modified system, and the DUKF successfully converges to the solutions for the system parameters while the UKF is not able to find some of the parameters accurately. Comparing the performance of these two techniques, application of the DUKF shows a significant improvement on identifying parameters, particularly those with varying identifiability within different branches, of the non-smooth system.

Concentrations of future work will be placed on the derivation of time-dependent healing process, and applying the observability and identification methods on the models of finite element.

References

1. M. Ismail, F. Ikhouane, J. Rodellar. 2009. The hysteretic bouc-wen model, a survey. Arch Comput Methods Eng; 16:161-188.
2. M.V. Sivaselvan, A. M. Reinhorn. 2000. Hysteretic models for deteriorating inelastic structures. Journal of Engineering Mechanics; 126:633–640.
3. J. Song, J. Pincheira. 2000. Spectral displacement demands of stiffness and strength degrading systems. Earthquake Spectra; 16:817–851.
4. J.L. Beck, L.S. Katafygiotis. 1998. Updating models and their uncertainties. i: Bayesian statistical framework. Journal of Engineering Mechanics; 124(4):455-461.

5. M.N. Chatzis, E.N. Chatzi, A.W. Smyth. 2014. An experimental validation of time domain system identification methods with fusion of heterogeneous data. Earthquake Engineering and Structural Dynamics;44(4):523-547.
6. S.P. Triantafyllou, M.N. Chatzis. 2015. A new damage-healing smooth hysteretic formulation for the modelling of self-healing materials. Proceedings of the 8th GRACM International Congress on Computational Mechanics, Volos.
7. S.P. Triantafyllou, E.N. Chatzi. 2014. A hysteretic multiscale formulation for nonlinear dynamic analysis of composite materials. Computational Mechanics; 54(3):763-787.
8. S.P. Triantafyllou, V.K. Koumousis, M.ASCE. 2014. Hysteretic finite elements for the nonlinear static and dynamic analysis of structures. Journal of Engineering Mechanics; 140(6): 04014025.
9. R. Hermann, A. Krener. 1977. Nonlinear controllability and observability. Automatic Control, IEEE Transactions; 22(5):728-740.
10. A. Sedoglavic. 2012. A probabilistic algorithm to test local algebraic observability in polynomial time. Journal of Symbolic Computation; 33:735-755.
11. M.N. Chatzis, E.N. Chatzi, A.W. Smyth. 2015. On the observability and identifiability of nonlinear structural and mechanical systems. Structural Control and Health Monitoring; 22:574-593.
12. M.N. Chatzis, E.N. Chatzi. 2017. A discontinuous unscented kalman filter for non-smooth dynamic problems. Frontiers in Built Environment. 3:56.
13. L.S. Katafygiotis, J.L. Beck. 1998. Updating models and their uncertainties. ii: model identifiability. Journal of Engineering Mechanics; 124(4):463-467.
14. A.F. Villaverde, A. Barreiro, A. Papachristodoulou. 2016. Structural Identifiability of Dynamic System Biology Models. Computational Biology 12(10).
15. M.N. Chatzis, E.N. Chatzi, S.P. Triantafyllou. 2017. A Discontinuous Extended Kalman filter for non-smooth dynamic problems. Mechanical Systems and Signal Processing. 92:13-29.
16. S.J. Julier, J.K. Uhlmann. A new extension of the Kalman filter to nonlinear systems. Proceedings of AeroSense: The 11th Int. Symposium on Aerospace/Defense Sensing, Simulation and Controls, Orlando.
17. D. Simon. 2006. Optimal State Estimation: Kalman, H-infinity and Nonlinear Approaches. John Wiley & Sons.
18. E.N. Chatzi, A. Smyth. 2009. The unscented kalman filter and particle filter methods for nonlinear structural system identification with non-collocated heterogeneous sensing. Structural Control and Health Monitoring; 16(1):99-123.